7.4 MAPPING SURFACE REFLECTIVE PROPERTIES OVER THE ARM SGP CART AREA BY COMBINING MULTI-PLATFORM OBSERVATIONAL DATASETS

Alexander P. Trishchenko*, Yi Luo, Rasim Latifovic, William Park, Josef Cihlar
Canada Centre for Remote Sensing, Ottawa, ON, Canada
Zhanqing Li
University of Maryland, MD, USA

1. INTRODUCTION

Surface albedo is a key variable determining the disposition of solar radiation between the surface and the atmosphere. Reliable mapping of surface albedo and improved understanding of radiation interactions at the surface are required for advancing weather forecasting and climate studies. The ground-based observations are limited to a handful of locations sparsely distributed in the South Great Plains (SGP). Frequently, they represent only small-scale features of surface reflective properties and may not be representative for larger scales. Satellite data combined with necessary field validation measurements are suitable source of such information. A major objective of this project is to develop a comprehensive database of surface spectral reflective properties at high resolution over the Atmospheric Radiation Measurement (ARM) Program's Southern Great Plains (SGP) Cloud And Radiation Testbed (CART) site, which is characterized by diverse surface conditions and strong seasonal variations. We are developing satellite data processing system aimed onto systematic generation of surface narrowband and broadband reflectance, albedo, as well as the normalized difference vegetation index (NDVI) and some other parameters over the Southern Great Plains area of ~10deg x 10deg on various time scales.

2. METHODOLOGY

We are attempting to map the spectral surface albedos at varying spatial resolution for different times of a year using all available datasets primarily from polar orbiting and geostationary satellite observations, combined with ground and aircraft measurements. The size of the mapping area is approximately 1000x1000 km^2, which encompasses the entire ARM SGP CART site. The satellite observations include various systems, such as AVHRR (Advanced Very High Resolution Radiometer), VEGETATION (VGT) on SPOT platform, MODIS (Moderate Resolution Imaging Spectroradiometer), and CERES (Clouds and the Earth's Radiant Energy System). Historical satellite data such as ERBE, ScaRaB and earlier AVHRR observation as well as high-resolution data from Landsat TM will be also processed. Available multi-angular observations are also considered, especially for validation of bi-directional surface properties derived from cross-track scanner data. The structure of database and data manipulation system is shown in Figure 1.

It has the following main functions: (1) compositing of clear-sky scenes from multiple satellite images; (2) removal of the atmospheric effect and cloud contamination; (3) bi-directional (BRDF) correction and normalization; (4) correction for surface-atmosphere radiative coupling; (5) adjustment to specific clear/cloudy sky conditions; and (6) scaling-up of pixel albedo to grid-cell albedo.

Clear-sky compositing approach and some other aspect of data processing is discussed by Cihlar et. al. (2002a, 2002b). Further, we discuss with more details atmospheric correction, parameterization of surface bi-directional properties and coupling between surface albedo and atmospheric radiation field.

3. DIRECTIONAL PROPERTIES OF SURFACE REFLECTANCE AND ALBEDO

The most complete description of surface reflective properties is achieved by means of bi-directional reflectance distribution function (BRDF) ρ (Nicodemus et al., 1977), which is a function of solar zenith angle θ_0, viewing zenith angle θ, relative azimuth ϕ, wavelength λ, spatial coordinate $\vec{X}$ and time t, that accounts for the seasonal changes of surface reflective properties:

$$\rho = \rho(\theta_0, \theta, \phi, \lambda, \vec{X}, t) \qquad (1)$$

The apparent spectral albedo of a surface is defined as ratio of upward and downward fluxes.

$$\alpha(\theta_0, \lambda) = \frac{F^{\uparrow}(\theta_o, \lambda)}{F^{\downarrow}(\theta_o, \lambda)} \qquad (2)$$

We omitted the dependence on spatial coordinate $\vec{X}$ and time t in Eq. (2).

Since upward surface flux $F^{\uparrow}$ is a convolution of BRDF function and downward radiance field in upward hemisphere, the albedo (2) depends on sky-conditions and, strictly speaking, is not an intrinsic property of the surface. It is a combined property of downwelling radiance field and shape of the surface BRDF function.

*Corresponding author address: A. P. Trishchenko, Canada Centre for Remote Sensing (CCRS), 588 Booth Str, Ottawa, ONT, K1A 0Y7 Canada, e-mail: trichtch@ccrs.nrcan.gc.ca

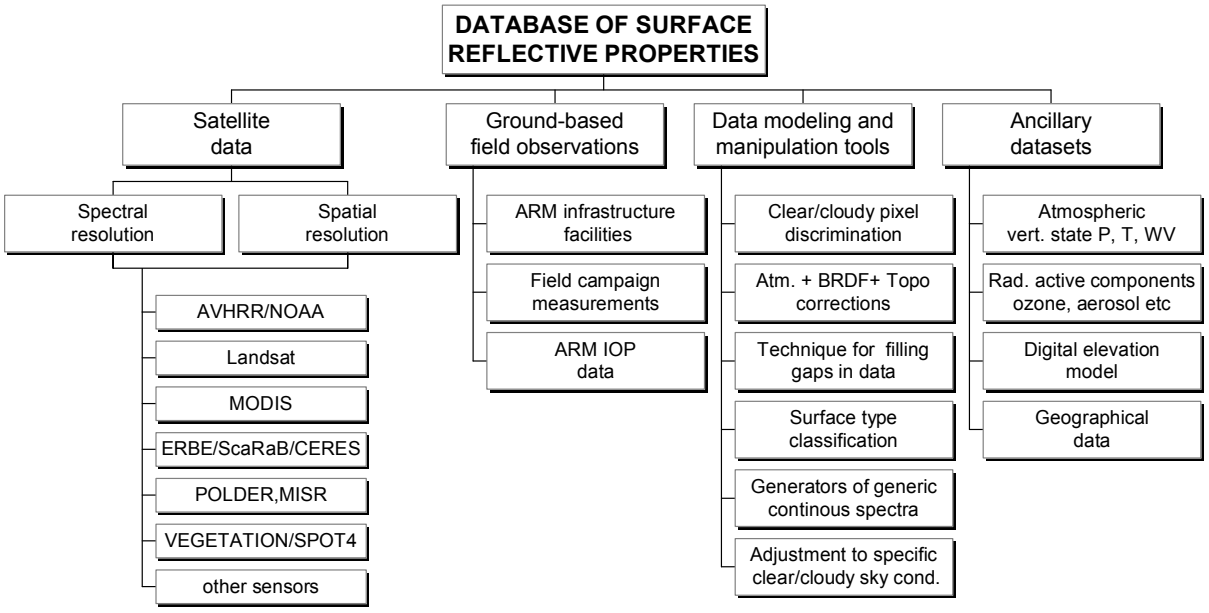

Fig.1 The structure of database of surface reflective properties

The albedos for wide spectral bands $\Delta\lambda = \lambda_2 - \lambda_1$ or broadband shortwave albedo are determined by a spectral convolution of downwelling flux and surface apparent albedo $\alpha(\theta_0, \lambda)$.

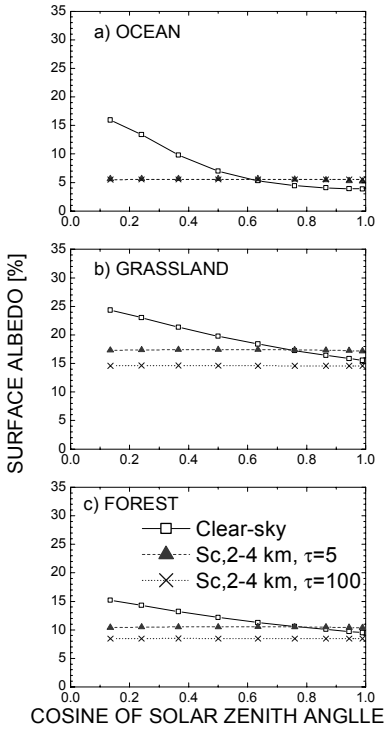

Fig.2. Dependence of surface albedo on atmospheric conditions.

$$\alpha_{\Delta\lambda}(\theta_0) = \frac{\int_{\lambda_1}^{\lambda_2} \alpha(\theta_0, \lambda) F^{\downarrow}(\theta_0, \lambda) d\lambda}{\int_{\lambda_1}^{\lambda_2} F^{\downarrow}(\theta_0, \lambda) d\lambda} \quad (3)$$

An example of coupling between surface BRDF properties and radiation field is presented in Figure 2, which shows broadband shortwave albedo for various surfaces and different atmospheric conditions.

One can define two functions that represent "true" surface albedo properties independent on sky-conditions: "black-sky" and "white-sky" albedos (Dickinson, 1983; Liang et al., 1999). The "black-sky" albedo is defined as

$$\alpha_{BS}(\theta_0, \lambda) = \frac{2}{\pi} \int_0^{\pi} d\phi \int_0^1 \mu \, d\mu \; \rho(\theta_0, \theta, \phi, \lambda). \quad (4)$$

It corresponds to idealized situation when no diffuse component of downwelling radiation at the surface level is present. This case approximately describes clear-sky conditions in "clean" atmosphere.

The "white-sky" albedo is defined as

$$\alpha_{WS}(\lambda) = 2 \int_0^1 \mu \, d\mu \, \alpha_{BS}(\mu_0, \lambda) \quad (5)$$

The case of white-sky albedo corresponds to idealized situation of isotropic diffuse radiation. This case is approximately describes the overcast conditions. In Eqs. (4-5) $\mu = \cos\theta$ and $\mu_0 = \cos\theta_0$. Above albedo quantities can be combined to provide a simple parameterization of the apparent surface albedo under real-sky conditions.

$$\alpha(\theta_0, \lambda) \approx T_{dir} \alpha_{BS}(\theta_0, \lambda) + (1 - T_{dir}) \alpha_{WS}(\lambda) \quad (6)$$

T_{dir} in (6) is a fraction of direct component of the total downward surface flux (Trishchenko et al., 2001).

4. APPROPRIATE SPATIAL RESOLUTION OF ALBEDO MAPPING FOR RADIATION STUDIES

Common sense tells us that for better characterization of surface properties one needs to use high-resolution imagery. This may be true for certain applications, like crop monitoring, land inventory, disaster monitoring etc. Obvious difficulty with this approach is a large volume of data, which is inversely proportional to image spatial resolution (inverse quadratic dependence). Another problem is a temporal coverage of the high-resolution imagery, which may not be adequate due to problems with cloud cover and large repetition period of the observations from high-resolution sensors. Do we really need the high-resolution imagery for the studies of solar radiation? If not, what is appropriate spatial resolution for albedo mapping?

Follow to Chandrasekhar's (1960) approach, one can write expression for downward radiation $F^{\downarrow}(\lambda,\vec{X})$ as

$$F^{\downarrow}(\lambda,\vec{X}) = \frac{F_0^{\downarrow}(\lambda)}{1-<\alpha(\lambda,\vec{X})>S}, \qquad (7)$$

where $F_o^{\downarrow}$ is a downward flux for the black surface ($\alpha(\lambda)=0$), S is a hemispherical albedo of the atmosphere, $<\alpha(\lambda,\vec{X})>$ is the areal mean albedo around point $\vec{X}$. Eq. (7) shows that the impact of surface albedo on downward radiation at point $\vec{X}$ is determined by the average surface properties of surrounding area. The size of the area is the largest for the clear-skies and smallest for cloudy conditions with low cloud bottom (Li et al., 2002). Typical size of the averaging area is estimated to be of the order of few kilometres and varies with sky conditions and atmospheric absorption at specific spectral band. As such, we conclude that the observations available from medium resolution sensors, such as AVHRR, VEGETATION/SPOT, MODIS and similar instruments, with pixel size ~1 x 1 km^2 provide adequate spatial representation of albedo for the atmospheric radiation applications.

5. ATMOSPHERIC CORRECTION

Atmospheric correction of satellite measurements is an important step in the retrieval of surface reflective properties. It involves removing the effect of gaseous absorption, as well as correcting for the effect of an atmospheric molecular and particulate scattering. Significant advance in our knowledge of the absorbing properties of various atmospheric radiatively active gases has been achieved in the past few years. In particular, Giver et al. (2000) reported an important updates to the parameters of line and continuum absorption by water vapour. These and other updates have been incorporated into HIRTRAN spectroscopic database and implemented in MODTRAN-4 radiative transfer model (Berk, Anderson, et al., 2001 and 1999). We used the latest version of MODTRAN-4 combined with updated HITRAN 2001 database (Rothman, et. al., 2001) to estimate the impact of these improvements on atmospheric correction of the signal in solar domain for various satellite sensors.

Generally, we found more atmospheric absorption with MODTRAN-4, than it was estimated with earlier MODTRAN models, as well as 5S and 6S models (Vermote et al., 1997). This is especially evident for narrowband channels located in near-IR part of solar spectrum in the vicinity of water vapour absorption band located around 0.94μm (Trishchenko et al., 2002a). For example, the correction to atmospheric transmittance in AVHRR near-IR ch.2 reached up to 12% depending on observational condition, relative to the one computed with 6S model (version 4). This deviation could cause biases in the retrieved surface reflectance up to 0.01 ~ 0.04, which leads to underestimation of normalized difference vegetation index (NDVI) up to 10% or more in terms of relative bias.

6. BRDF PARAMETERIZATION

Following experimentation with various approaches, we adopted a model described by Latifovic et al. (2002):

$$\Lambda(\theta_s,\theta_v,\phi) = [1 + A(V) f_1(\theta_0,\theta,\phi) + B(V) f_2(\theta_0,\theta,\phi)][1 + Ce^{-\frac{\xi}{\pi}D}] \qquad (8)$$

where ξ is the scattering angle, f_1, f_2 are the kernel functions, V is Normalized Difference Vegetation Index, A and B are the second order polynomials of V. Coefficients C and D are constants. Using vegetation index V as input parameter allows us to account for the temporal changes in the state of vegetation. Last term in Eq. (8) serves for better parameterization of hot-spot effects. All parameters in (8) are spectral band and land cover type dependent.

7. COMBINING MULTIPLE SATELLITE DATASETS

Accurate description of surface bi-directional properties is critical for determination of surface albedo. Cross-track scanners provide a limited opportunity for reliable retrieval of BRDF shape, due to limited range of observational geometrical conditions (Trishchenko et al., 2001). We propose an approach to combine clear-sky data from several spaceborne instruments to produce more accurate estimates of BRDF parameters. This approach allows us to increase the number of clear-sky pixels involved in data processing, as well as significantly improve quality of the data fitting due to expanded range of angular variables. To make observations from different sensors consistent with each other, one needs to apply procedure of spectral adjustment. Details of this procedure are given by Trishchenko et al., 2002b.

An example of data processing is presented in Figure 3 that shows NDVI image over the SGP area

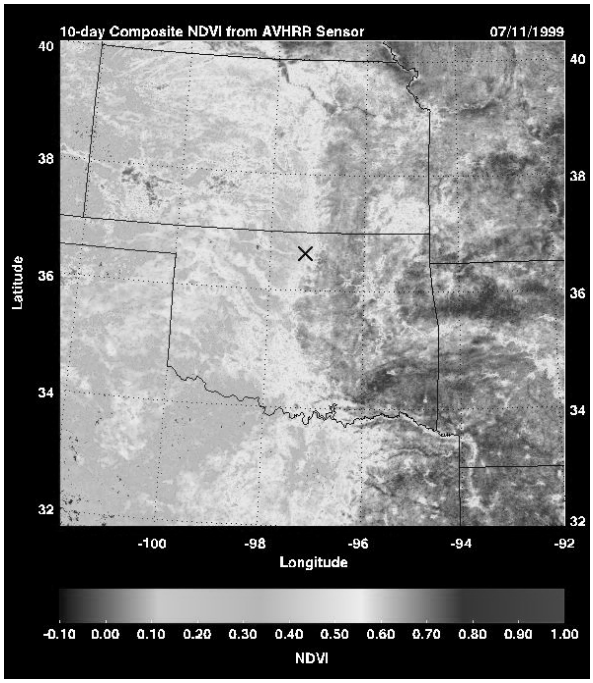

Fig. 3. NDVI over SGP area derived from normalized AVHRR observations.

derived from the AVHRR/NOAA-14 data for the period of July 11-20, 1999.

The image shows NVDI derived from ch.1 and 2 reflectances normalized to standard geometry (θ_0 =45^O, θ =0^O, ϕ =0^O) using BRDF function (8).

8. SUMMARY

An approach for systematic mapping of surface reflective properties and albedo over the ARM SGP CART area from multiple satellite observations is presented. Basic data processing steps, such clear-sky compositing, atmospheric correction, BRDF parameterization and albedo derivation are described. Paper discusses also a coupling between surface albedo and atmospheric radiation field. Some arguments in support of adequacy of medium-resolution sensors for mapping surface albedo are considered.

Acknowledgements. This research was supported by the US Department of Energy Atmospheric Radiation Measurement (ARM) Program, grant No. DE-FG02-02ER63351.

9. REFERENCES

Berk A., G.P. Anderson, P. K. Acharya, J. H. Chetwynd, L. S. Bernstein, E. P. Shettle, M. W. Matthew, and S. M. Adler-Golden, 2001: MODTRAN4 Version 2 User's manual. Air Force Research Laboratory. Space Vehicles Directorate. Air Force Materiel Command. Hanscom AFB, MA 01731-3010. 98pp .

Giver, L. P., C. Chackerian, Jr., and P. Varanasi, 2000: Visible and near-infrared H2 16 O line intensity corrections for HITRAN-96. *J. Quan. Spectr. Rad. Trans.,* 66, 101-105.

Chandrasekhar, S, 1960: Radiative transfer. Dover Publications Inc. 393p.

Cihlar, J., R. Latifovic, J. Chen, A. Trishchenko, Y. Du, G. Fedosejevs, and B. Guindon, 2002a: Systematic corrections of AVHRR image composites for temporal studies. *Rem. Sens. Environ*. In press.

Cihlar, J., J. Chen, Z. Li, R. Latifovic, G. Fedosejevs, M. Adair, W. Park, R. Fraser, A. Trishchenko, B. Guindon, D. Stanley, D. Morse, 2002b:. GeoComp N, an advanced system for the processing of coarse and medium resolution satellite data. *Can. J. Rem. Sensing*. 28, 21-44

Dickinson, R. E., 1983: Land surface processes and climate-surface albedos and energy balance. *Adv. Geophys*. 25, Academic Pess. 305-353.

Latifovic, R., J. Cihlar, J. Cheng, 2002: A comparison of BRDF models for the normalization of satellite optical data to a standard sun-target-sensor geometry. *IEEE Trans. Geosci. Remote Sens*. In press.

Liang, S., A. H. Strahler, C. Walthall, 1999 : Retrieval of land surface albedo from satellite observations: A simulation study. *J. App. Meteorol*., 38, 712-725.

Li, Z., M. Cribb, A. Trishchenko, 2002: Impact of surface inhomogeneity on the closure of solar radiative transfer and a method of estimating surface areal-mean albedo from downwelling flux measurements. *J. Geophys. Res.* 2002. In press.

Nicodemus, F. E., J. C. Richmond, J. K. Hsia, I. W. Ginsberg, and T. Limperis, 1977: in *Geometrical Consideration and Nomenclature for Reflectance, Natl. Bur. of Stand. Monogr*., 160, Washington, D.C.

Trishchenko A. P., B. Hwang, Z Li, 2002a: Atmospheric correction of satellite signal in solar domain: Impact of improved molecular spectroscopy. *Proc. 12th ARM Science Team Meeting*, Florida, (http://www.arm.gov/docs/documents/technical/conf_0204/trishchenko-ap.pdf)

Trishchenko A. P., J. Cihlar, Z. Li, 2002b: Effects of spectral response function on surface reflectance and NDVI measured with moderate resolution satellite sensors. *Rem. Sens. Environ*. 81, 1-18.

Trishchenko, A. P., Z. Li, W. Park, J. Cihlar, 2001: Corrections for the BRDF and topographic effects in satellite retrieval of surface spectral reflectance in solar spectral region. In: W. L. Smith, & Y. Tymofeyev (Eds.*), Proc. of the Int. Radiation Symp. IRS 2000.* St. Petersburg, Russia, August 2000, vol. 147 pp. 44–47. Hampton, VA, USA: A. Deepak Publishing.

Vermote, E., D. Tanré, J. L. Deuzé, M. Herman, and J.-J. Morcette, 1997: Second simulation of the satellite signal in the solar spectrum: An overview. *IEEE Trans. Geosci. Remote Sens., 35,* 675-686.